

## EFFECT OF THE SIZE OF GRADED BAFFLES ON THE PERFORMANCE OF CHANNEL HEAT EXCHANGERS

by

**Djamel SAHEL<sup>a</sup>, Houari AMEUR<sup>b\*</sup>, and Touhami BAKI<sup>c</sup>**

<sup>a</sup> Technical Sciences Department, University of Amar Telidji, Laghouat, Algeria

<sup>b</sup> Institute of Science and Technology, University Center of Naama (Ctr Univ Naama), Naama, Algeria

<sup>c</sup> Mechanical Engineering Department, University of science and the technology, Oran, Algeria

Original scientific paper

<https://doi.org/10.2298/TSCI180326295S>

*The baffling technique is well-known for its efficiency in terms of enhancement of heat transfer rates through channels. However, the baffles insert is accompanied by an increase in the friction factor. This issue remains a great challenge for the designers of heat exchangers. To overcome this issue, we suggest in the present paper a new design of baffles which is here called graded baffle-design. The baffles have an up- or down-graded height along the channel length. This geometry is characterized by two ratios: up-graded baffle ratio and down-graded baffle ratio which are varied from 0-0.08. For a range of Reynolds number varying from  $10^4$  to  $2 \times 10^4$ , the turbulent flow and heat transfer characteristics of a heat exchanger channel are numerically studied by the computer code FLUENT. The obtained results revealed an enhancement in the thermohydraulic performance offered by the new suggested design. For the channel with a down-graded baffle ratio equal to 0.08, the friction factors decreased by 4-8%.*

**Key words:** heat exchanger channel, graded baffles, turbulent flow, friction factor, CFD

### Introduction

Several techniques are developed to reduce the energy cost and to enhance the thermal performance of various devices used in many industrial applications. In this framework, ribs, baffles or obstacles play an important role in for the improvement of the thermal transfer rate in various thermal systems like the heat exchangers, the gas turbines blades, the solar collectors, the car radiators and other applications of fluids mechanics such as the water desalination.

Some experimental and numerical works have been achieved on the effect of different geometrical parameters of baffles as the shape, size and spacing between baffles, the attack angle, the blockage ratio (BR) and the porous space. The shape of baffles is a necessary parameter for the generation of vortices [1-3]. Therefore, various shapes have been developed, for example, the *V*-baffle shape [4-9], the *W*-baffle shape [10], the *Z*-baffle shape [11], multi *V*-type perforated baffles [12-17] and diamond shape proposed by Sripattanapipat and Promvong [18]. All these shapes permit an enhancement in the heat transfer rates, but with catastrophic pressure drops. Dutta et Hassain [19] studied by experiments the effect of baffle attack angle on the characteristics of heat transfer and pressure drop in a rectangular channel with inclined plate and perforated baffles. They showed the main dependency of the thermal transfer rates on the geometry, the orien-

\* Corresponding author, e-mail: houari\_ameur@yahoo.fr

tation and the position of the second baffle. For a square channel Promvong and Thianpong [20] explored the effect of baffle inclination with various values of BR. With the  $45^\circ$  inclined baffles and  $BR = 0-0.05$ , they found an increase in the thermal transfer rate from 150-850% accompanied with pressure losses varying from 2 to 70 times compared with the smooth channel. In other works [21, 22], these authors found that the combination between the attack angle and the  $V$ -baffle shape allow an enhancement in heat transfer rates associated with losses in pressure. In the same framework, Promvong *et al.* [23] studied by experiments the effects of the delta baffles shapes on the thermal performance of solar air heater. They reported that the combination between the delta winglet and the rib ensures considerable heat transfer improvements ( $Nu/Nu_0 = 2.3-2.6$ ) and also yields a moderate pressure drop increase ( $f/f_0 = 4.7-10.1$ ).

Tandiroglu and Ayhan [24] explored in their experimental study three cases of inclined baffles ( $45^\circ$ ,  $90^\circ$ , and  $180^\circ$ ) with three values of diameter ratio  $H/D = 1, 2$ , and  $3$  and they obtained the best performance with the  $90^\circ$  case for the forced convection. In another work, Tandiroglu [25] developed empirical formulas for the calculation of Nusselt numbers and the friction coefficients. The same author, tested in another article the entropy generation for different types of baffles [26].

The  $V$ -shaped baffle or rib is another technique to enhance the thermal performance due to the presence of two high thermal regions. Some researcher [27, 28] reported that the staggered arrangement of ribs gives less higher heat transfer coefficient than the symmetric arrangement ribs. Further studies on the enhancement of heat transfer by the baffling technique can be found elsewhere [29-32].

The efficiency of porous baffles is confirmed by many researchers because the perforated space enables the agitation of the flow stagnated behind of baffles [33, 34], it increases the thermal transfer intensity and eliminates the lowers heat transfer areas (LHTA) [35-38]. All studies in literature confirm that the baffling technique increases significantly the heat transfer rates. However, these works did not correct the major problems of this technique: the formation of LHTA and the pressure losses.

Aiming to reduce the friction factor in baffled channels, we propose here new designed baffles with up-graded and down-graded height along the channel length. The performance of the new design has been investigated for different flow rates.

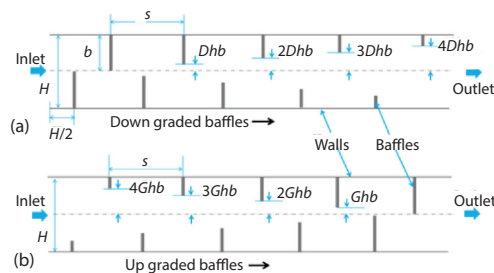


**Figure 1. Geometry of the problem studied;**  
**(a) down-graded baffles, (b) up-graded baffles**

### Geometry of the problem studied

The purpose of the present work is to study the flow and heat transfer characteristics in a horizontal channel with a baffle series of up- and down-graded height along the channel length,  $L$ . The baffles are inserted in a staggered array on the upper and lower walls of the channel, fig. 1. Variations in the baffle height are defined by DBR, fig. 1(a) and GBR, fig. 1(b) for the decreased (*i. e.* down-graded) and increased (*i. e.* up-graded) baffle ratios, respectively.

The obtained results from the baffled cases are compared with those for a smooth channel (without baffles) having the following geometrical parameters:  $H$  – the channel height fixed to  $0.1$  m,  $b$  – the baffle height,  $e$  – the baffle thickness.  $e = 0.02 H$ , and  $b/H$  – is known as the BR. The spacing ratio between baffles is  $S = s/H = 1$ . Effects of DBR and GBR where investigated by changing their values for  $0-0.08$ .

**Mathematical formulation**

The numerical model for heat transfer and fluid-flow in the 2-D channel is based on the previous assumptions. The flow through the duct is governed by the RANS equation [39] and the energy equation:

– continuity equation

$$\frac{\partial}{\partial x_i}(\rho u_i) = 0 \tag{1}$$

– momentum equation

$$\frac{\partial}{\partial x_i}(\rho u_i u_j) = \frac{\partial}{\partial x_i} \left[ \mu \left( \frac{\partial u_i}{\partial x_j} - \overline{\rho u'_i u'_j} \right) \right] - \frac{\partial P}{\partial x_i} \tag{2}$$

where  $u'$  is a fluctuating component of velocity.

– energy equation

$$\frac{\partial}{\partial x_i}(\rho u_i T) = \frac{\partial}{\partial x_i} \left( (\Gamma + \Gamma_t) \frac{\partial T}{\partial x_j} \right) \tag{3}$$

where  $\Gamma$  is the molecular thermal diffusivity given by  $\Gamma = \mu/\text{Pr}$ ,  $\Gamma_t$  – the turbulent thermal diffusivity given by  $\Gamma_t = \mu_t/\text{Pr}_t$ .

The Reynolds-averaged approach to turbulence model requires the modelling of Reynolds stresses  $\overline{\rho u'_i u'_j}$  in eq. (2). The Boussinesq hypothesis relates the Reynolds stresses to the mean velocity gradients:

$$\overline{\rho u'_i u'_j} = \mu_t \left( \frac{\partial u_i}{\partial x_j} + \frac{\partial u_j}{\partial x_i} \right) - \frac{2}{3} \left( \rho k + \mu_t \frac{\partial u_i}{\partial x_i} \right) \delta_{ij} \tag{4}$$

where  $k$  is the turbulent kinetic energy defined by,  $k = 1/2 \overline{u'_i u'_i}$  and  $\delta_{ij}$  is the Kronecker delta. The RNG-based  $k$ - $\epsilon$  turbulence model is derived from the instantaneous Navier-Stokes equations [39], using a mathematical technique called renormalization group (RNG) methods. The steady-state transport equations are expressed:

$$\frac{\partial}{\partial x_j}(\rho k u_i) = \frac{\partial}{\partial x_j} \left[ \left( \mu + \frac{\mu_t}{\sigma_k} \right) \frac{\partial k}{\partial x_j} \right] + G_k + \rho \epsilon \tag{5}$$

$$\frac{\partial}{\partial x_i}(\rho \epsilon u_i) = \frac{\partial}{\partial x_j} \left[ \left( \mu + \frac{\mu_t}{\sigma_\epsilon} \right) \frac{\partial \epsilon}{\partial x_j} \right] + C_{1\epsilon} \frac{\epsilon}{k} - C_{2\epsilon} \rho \frac{\epsilon^2}{k} \tag{6}$$

where  $G_k$  is the rate of generation of the  $k$ - $\epsilon$  model  $C_{1\epsilon}$  and  $C_{2\epsilon}$  are constants,  $\mu_t$  – the turbulent viscosity defined by  $\mu_t = \rho C_\mu (k^2/\epsilon)$ ,  $C_\mu$  is a constant set to 0.0845 and derived using the RNG theory.

The friction factor  $f$  is calculated by the following equation:

$$f = \frac{2}{L} \frac{\Delta P}{\rho U^2} \tag{7}$$

where  $\Delta P$  is the pressure drop across the length of the channel  $L$ .

To determine the heat transfer characteristics, we define the local Nusselt number:

$$\text{Nu}_x = \frac{h_x D_x}{k_f} \tag{8}$$

and the average Nusselt number:

$$\overline{Nu}_x = \frac{1}{A} \int Nu_x \partial A \quad (9)$$

The thermal enhancement factor  $\eta$  is defined:

$$\eta = \frac{\frac{Nu}{Nu_0}}{\left(\frac{f}{f_0}\right)^{1/3}} \quad (10)$$

where  $Nu_0$  and  $f_0$  stand for Nusselt number and friction factor for the smooth channel, respectively.

### Numerical simulation

#### Boundary conditions

Air was used as a working fluid in all cases with a uniform inlet temperature (300 K,  $Pr = 0.7$ ). Impermeable boundary and no-slip wall conditions have been implemented over the channel wall as well as the baffle. The temperature of the bottom and upper plates is maintained constant at 330 K while the baffle is assumed as adiabatic wall condition. The Reynolds number is changed from 10000-20000.

#### Grid generation

Geometry and mesh of the computational domain were created with the computer tool GAMBIT. The mesh generated is quadrilateral with regular grid elements. Mesh tests were realized by a series of grid selected in the unbauffed channel 25608, 36100, 40200, 59015, and 71112 elements. From the mesh with 40200 elements, the deviation of the Nusselt number is not important (do not exceed 2%) with the raise of the grid density. Thus and for the next calculations, the final selected grid number had 40200 elements. Using the same approach for the other cases with baffles, the selected grids were varied between 37000 and 39500 elements. The necessary details on mesh test are resumed on tab. 1.

**Table 1. Tests of grid sensivity for all configuratons**

|                   | Test 1 |        | Test 2 |        | Test 3 |        | Test 4 |        | Test 5 |        |
|-------------------|--------|--------|--------|--------|--------|--------|--------|--------|--------|--------|
|                   | Grid 1 | Nu     | Grid 2 | Nu     | Grid 3 | Nu     | Grid 4 | Nu     | Grid 5 | Nu     |
| Smooth channel    | 25608  | 29.17  | 36100  | 19.28  | 40200  | 48.8   | 59015  | 49.10  | 71112  | 48.16  |
| <i>DBR</i> = 0.02 | 25788  | 162.35 | 37254  | 212.36 | 39554  | 305.49 | 60002  | 308.19 | 73254  | 307.88 |
| <i>DBR</i> = 0.04 | 24772  | 190.00 | 36992  | 119.24 | 39490  | 281.09 | 59322  | 278.01 | 70786  | 278.92 |
| <i>DBR</i> = 0.06 | 26710  | 122.89 | 35998  | 252.10 | 38112  | 273.77 | 58088  | 274.14 | 71250  | 272.63 |
| <i>DBR</i> = 0.08 | 25718  | 198.58 | 34048  | 212.12 | 38586  | 267.42 | 61002  | 269.78 | 73254  | 268.55 |
| <i>GBR</i> = 0.02 | 23711  | 50.11  | 36254  | 201.33 | 39554  | 314.76 | 60997  | 313.44 | 69011  | 313.78 |
| <i>GBR</i> = 0.04 | 24111  | 141.88 | 37982  | 252.02 | 38999  | 310.32 | 52049  | 308.19 | 65114  | 307.93 |
| <i>GBR</i> = 0.06 | 24352  | 197.28 | 37449  | 199.78 | 39500  | 314.75 | 58021  | 314.77 | 66194  | 313.58 |
| <i>GBR</i> = 0.08 | 24228  | 98.39  | 36229  | 177.99 | 38511  | 310.48 | 48049  | 313.13 | 62004  | 312.82 |

Computations were achieved with the CFD FLUENT, which is based on the method of finite volume to solve the governing equations. The flow regime is considered as turbulent and steady-state.

The QUICK numerical scheme coupled with the semi-implicit pressure linked equation (SIMPLE) algorithm were used in the finite volume method to solve all equations. The RNG  $k-\varepsilon$  model was employed for the closure of the equations. Default under-relaxation factors of the solver are used to control the update of computed variables at each iteration. These factors are: 0.3, 1, 0.7, and 1 for pressure, density, momentum, and energy, respectively. Solutions were considered converged when the normalized residual values were below  $10^{-5}$  for all variables and below  $10^{-7}$  only for the energy equation.

## Results and discussion

### Verification of results for a smooth channel

Our predicted results for the Nusselt number and friction factor through a smooth channel are, respectively, compared with Dittus-Boelter and Blasius correlations. These correlations, which are used by for the characterization of fluid-flow and heat transfer in ducts [24], are available in the literature [40]:

$$Nu = 0.023 Re_{D_h}^{0.8} Pr^{0.4} \quad (13)$$

$$f_0 = 0.0791 Re^{-0.25} \quad (14)$$

Figures 2(a) and 2(b) show, respectively, a comparison of Nusselt number and friction factor obtained from the present study with those from eqs. (11) and (12). In these figures, the presented results agree reasonably well within  $\pm 2.9\%$  and  $\pm 5.5\%$  for both friction factor correlation of Blasius and Nusselt number correlation of Dittus-Boelter, respectively.

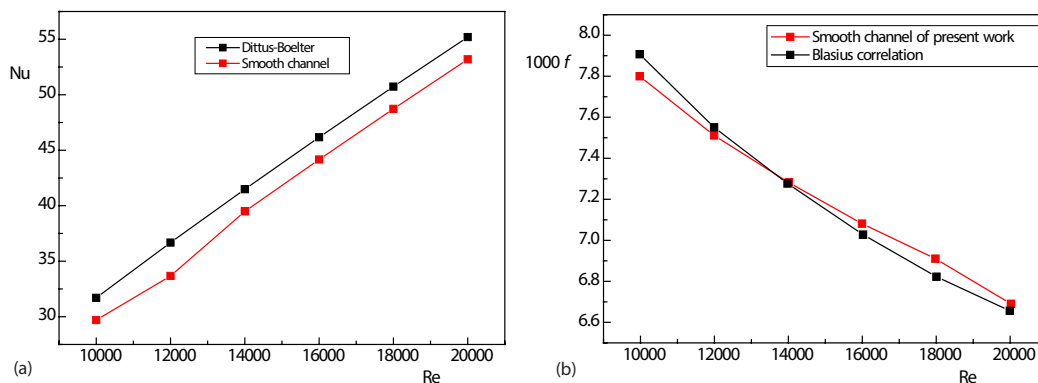


Figure 2. Verification of (a) Nusselt number and (b) friction factor for a smooth channel

### Flow Structure

For  $Re = 18000$  and  $S = 1$ , the axial velocity is presented on fig. 3 for  $DBR = 0.08$ ,  $DBR = 0.04$ ,  $DBR/GBR = 0$ ,  $GBR = 0.04$ , and  $GBR = 0.08$ . This figure shows the aerodynamic nature of the flow in the presence of baffles with down- and up-graded height. At the baffle, the flow is separated in three zones: a zone of recirculated flow behind the baffles where the vortex appears clearly. The second zone is located in front of the first zone where the axial velocity is very intense, and the third zone is located between the first and the second zones where the flow

passes with a mean velocity. This aerodynamic phenomenon depends on the size of baffles and the direction of changes in their height (up- or down-graded height). Consequently, this figure shows that the raise of  $DBR/GBR$  decreases the formation of the vortex structures.

The effect of down- and up-graded size of baffles on the formation of vortex is illustrated in fig. 3. The formation of the vortex is clearly appearing in the case of channel with down-graded size of baffle  $DBR = 0.08$  and  $0.04$ . On the other hand, the vortex size in the case of channel with up-graded size of baffle  $GBR = 0.08$  and  $0.04$  is small compared with  $DBR = 0.08$  and  $0.04$ , respectively. This phenomenon is due to the development of the flow along the channel in the presence of baffles. Consequently, the down-graded size of baffle ensures further intensified vortices despite of the reduction of baffles size ( $DBR = 0.08$ ). Therefore, the weaker vortex is observed with the case  $GBR = 0.08$ , because that the small baffles located at the entrance of channel do not allow an efficient developed flow.

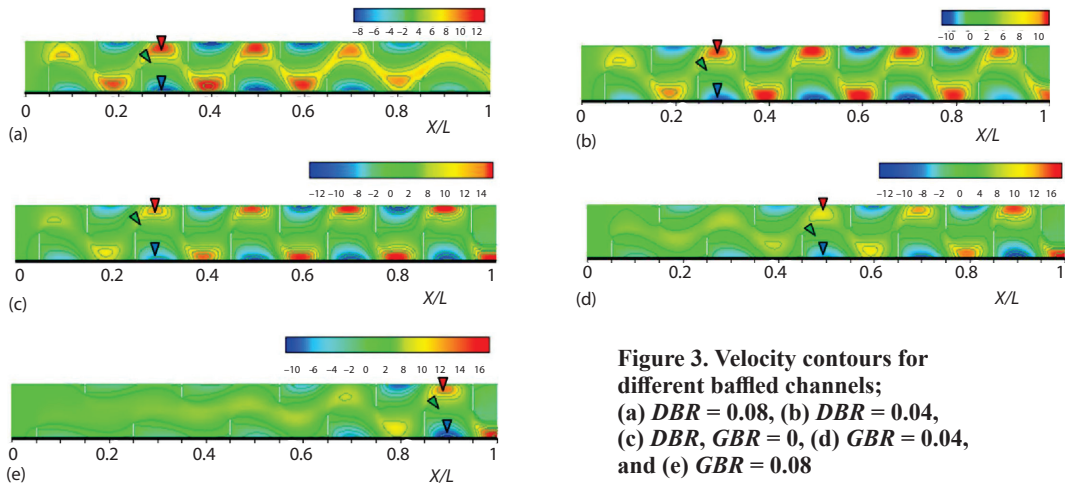


**Figure 3. Velocity contours for different baffled channels; (a)  $DBR = 0.08$ , (b)  $DBR = 0.04$ , (c)  $DBR, GBR = 0$ , (d)  $GBR = 0.04$ , and (e)  $GBR = 0.08$**

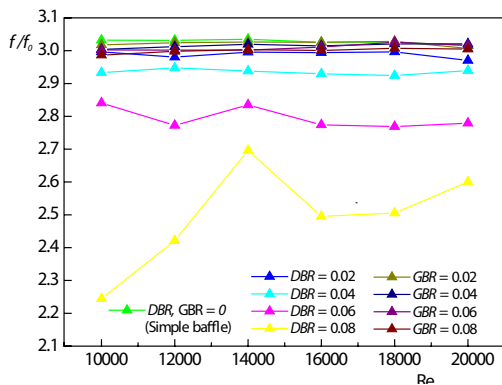


**Figure 4. Variation of  $f/f_0$  with Reynolds number for various baffled channels**

### Pressure losses

Figure 4 presents the variation of the normalized friction factor,  $f/f_0$  with Reynolds number values for different  $GBR$  and  $DBR$ . As shown on this figure, the use of down-/up-graded height of baffle leads to a considerable decrease in the friction factor compared with the simple baffles ( $GBR, DBR = 0$ ). The  $DBR$  values present further increases in the friction factor compared with  $GBR$  values. Depending on Reynolds number, the lowest value of friction factor is obtained with  $DBR = 0.08$ , which is considered to be smaller by about 4-8% than that of a simple baffle channel.

### Heat transfer

At  $Re = 18000$ , the axial variation of Nusselt number along the lower channel wall is presented on fig. 5 for different values of  $DBR/GBR$ . The following phenomena can be observed:

- the weak thermal transfer rate remarked on the basis of baffle, and particularly behind it, is caused by the formation of hot pockets in this region,
- the highest thermal transfer rates are observed in the zones where the flow is reattached (*i. e.* which between two successive baffles), and
- the simple baffle allows the highest thermal transfer rates. However, the case  $GBR = 0.08$  gives the lowest heat transfer rates.

For a simple baffle,  $S = 1$  and  $BR = 0.5$ , variations of the average  $Nu/Nu_0$  ratio with Reynolds number for different down-/up-graded heights of baffles are presented on fig. 6. This figure shows that the  $Nu/Nu_0$  value increases with the raise of Reynolds number values for all  $GBR$  and  $DBR$  cases. The use of simple baffle ensures a good thermal transfer rate and the baffles with  $GBR = 0.02$  reduces the heat transfer rate by 5% compared with the simple baffle. The lowest thermal transfer rate which is given by the  $DBR = 0.08$  tends to 16% compared with the simple baffle.

Figure 7 shows the variation of the thermal enhancement factor,  $\eta$ , with Reynolds number for different down-/up-graded heights of baffles. The enhancement factor tends to increase with the raise of Reynolds number for all cases. The cases of  $GBR = 0.02$  and simple baffle ( $GBR = 0$ ) present the same best enhancement factors,  $\eta$ , up to 3.6 times at the highest value of Reynolds number.

### Conclusion

The turbulent flow and heat transfer characteristics in a 2-D channel equipped with down-/up-graded height of baffles have been explored numerically. The predicted results confirm that the new design of baffles provides an adequate reduction in friction factors. Depending on Reynolds number, the case of  $DBR = 0.08$  presents the minimum value of friction factor which is about 4-8% less than that of the simple baffled channel ( $DBR, GBR = 0$ ). However, the friction factor reduction is associated with a reduction in heat transfer rates tends to 5% as a maximum value compared with the simple baffled channel.

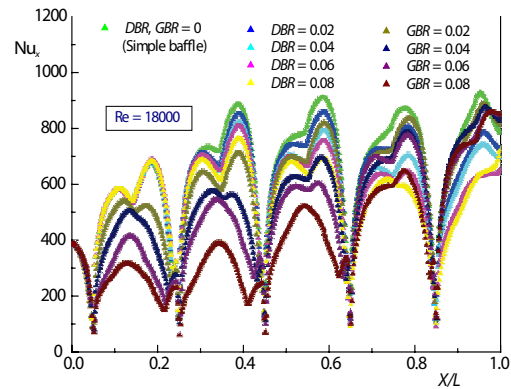


Figure 5. Axial variation of  $Nu_x$  along lower channel wall for various baffled channels,  $Re = 18000$

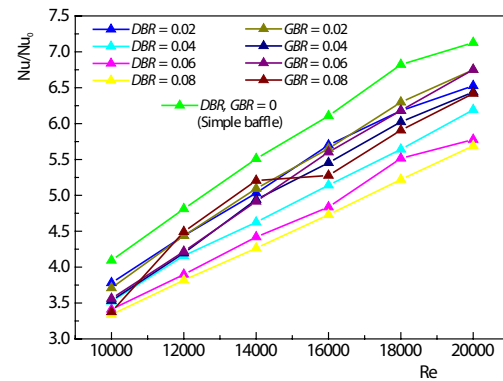


Figure 6. Variation of  $Nu/Nu_0$  with Reynolds number for various baffled channels

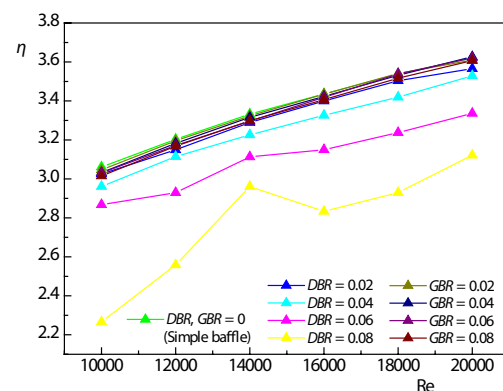


Figure 7. Thermal enhancement factor for various baffled channels

## Nomenclature

|          |  |
|----------|--|
| $b$      | – simple baffle height, [m]                                    |
| $D$      | – hydraulic diameter, [m]                                      |
| $D_{hb}$ | – down-graded height of baffle [m]                             |
| $f$      | – friction factor, [–]   |
| $h$      | – heat transfer coefficient, [ $\text{Wm}^{-2}\text{K}^{-1}$ ] |
| $H$      | – channel height, [m]  |
| $G_k$    | – turbulent kinetic energy production                          |
| $G_{hb}$ | – up-graded height of baffle, [m]                              |
| $k$      | – turbulent kinetic energy, [ $\text{m}^2\text{s}^{-2}$ ]      |
| $k_f$    | – thermal conductivity, [ $\text{Wm}^{-1}\text{K}^{-1}$ ]      |
| $L$      | – channel length, [m]  |
| $Nu$     | – Nusselt number   |
| $Re$     | – Reynolds number, ( $= \rho u D / \mu$ )                      |
| $S$      | – spacing ratio ( $= s/D$ )                                    |
| $T$      | – temperature, [K]   |
| $u$      | – mean velocity at the channel, [ $\text{ms}^{-1}$ ]           |

## Greek Letter

|               |   |
|---------------|---|
| $\varepsilon$ | – turbulent energy dissipation                          |
| $\mu$         | – dynamic viscosity, [ $\text{kgm}^{-1}\text{s}^{-1}$ ] |
| $\eta$        | – thermal enhancement factor, [–]                       |
| $\rho$        | – density, [ $\text{kgm}^{-3}$ ]                        |

## Subscripts

|     |                  |
|-----|------------------|
| $i$ | – $x$ -direction |
| $j$ | – $y$ -direction |

## Abbreviations

|     |   |
|-----|---|
| BR  | – blockage ratio ( $= b/D$ )                |
| DBR | – down-graded baffle ratio ( $= D_{hb}/H$ ) |
| GBR | – up-graded baffle ratio ( $= G_{hb}/H$ )   |

## References

- [1] Turgut, O., Arslan, K., Periodically Fully Developed Laminar Flow and Heat Transfer in a 2-D Horizontal Channel With Staggered Fins, *Thermal Science*, 21 (2017), 6, pp. 2443-2455
- [2] Turgut, O., Arslan, K., Periodically Fully Developed Laminar Flow and Heat Transfer in a 2-D Horizontal Channel with Staggered Fins, *Thermal Science*, 21 (2017), 6A, pp. 2443-2455
- [3] Kumar, R., et al., Experimental Investigation on Overall Thermal Performance of Fluid-flow in a Rectangular Channel with Discrete V-Pattern Baffle, *Thermal Science*, 22 (2018), 1, pp. 183-191
- [4] Lee, D. H., et al., Detailed Measurement of Heat/Mass Transfer With Continuous and Multiple V-Shaped Ribs in Rectangular Channel, *Energy*, 34 (2009), 11, pp. 1770-1778
- [5] Peng, W., et al., Experimental and Numerical Investigation of Convection Heat Transfer in Channels with Different Types of Ribs, *Applied Thermal Engineering*, 31 (2011), 14-15, pp. 2702-2708
- [6] Promvongse, P., et al., Numerical Heat Transfer Study of Turbulent Square-Duct Flow Through Inline V-Shaped Discrete Ribs, *International Communications in Heat and Mass Transfer*, 38 (2011), 10, pp. 1392-1399
- [7] Promvongse, P., et al., 3-D Simulation of Laminar Flow and Heat Transfer in V-Baffled Square Channel, *International Communications in Heat and Mass Transfer*, 39 (2012), 1, pp. 85-93
- [8] Hans, V. S., et al., Heat Transfer and Friction Factor Correlations for a Solar Air Heater Duct Roughened Artificially with Multiple V-Ribs, *Solar Energy*, 84 (2010), 6, pp. 898-911
- [9] Singh, S., et al., Exergy Based Analysis of Solar Air Heater Having Discrete V-Down Rib Roughness on Absorber Plate, *Energy*, 37 (2012), 1, pp. 749-758
- [10] Lanjewar, A., et al., Heat Transfer and Friction in Solar Air Heater Duct with W-Shaped Rib Roughness on Absorber Plate, *Energy*, 36 (2011), 7, pp. 4531-4541
- [11] Srirromreun, P., et al., Experimental and Numerical Study on Heat Transfer Enhancement in a Channel with Z-Shaped Baffles, *International Communications in Heat and Mass Transfer*, 39 (2012), 7, pp. 945-952
- [12] Kumar, A., Kim, M. H., Thermal Hydraulic Performance in a Solar Air Heater Channel with Multi V-Type Perforated Baffles, *Energies*, 9 (2016), 7, 564
- [13] Kumar, R., et al., Experimental Study and Correlation Development for Nusselt Number and Friction Factor for Discretized Broken V-Pattern Baffle Solar Air Channel, *Experimental Thermal and Fluid Science*, 81 (2016), 2, pp. 56-75
- [14] Kumar, R., et al., Experimental Study of Heat Transfer Enhancement in a Rectangular Duct Distributed by Multi V-Perforated Baffle of Different Relative Baffle Width, *Heat and Mass Transfer*, 53 (2017), 4, pp. 1289-1304
- [15] Kumar, R., et al., Experimental Study of Enhancement of Heat Transfer and Pressure Drop in a Solar Air Channel with Discretized Broken V-Pattern Baffle, *Renewable Energy*, 101 (2017), 2, pp. 856-872
- [16] Kumar, A., et al., Developing Heat Transfer and Pressure Loss in an Air Passage with Multi Discrete V-Blockages, *Experimental Thermal and Fluid Science*, 84 (2017), 6, pp. 266-278

- [17] Sharma, A., et al., Optimizing Discrete V Obstacle Parameters Using a Novel Entropy-VIKOR Approach in a Solar Air-flow Channel, *Renewable Energy*, 106 (2017), 6, pp. 310-320
- [18] Sripattanapipat, S., Promvong, P., Numerical Analysis of Laminar Heat Transfer in a Channel with Diamond-Shaped Baffles, *International Communications in Heat and Mass Transfer*, 36 (2009), 1, pp. 32-38
- [19] Dutta, P., Hossain, A., Internal Cooling Augmentation in Rectangular Channel Using Two Inclined Baffles, *International Journal of Heat and Fluid-Flow*, 26 (2005), 2, pp. 223-232
- [20] Promvong, P., Thianpong, C., Thermal Performance Assessment of Turbulent Channel Flows over Different Shaped Ribs, *International Communications in Heat and Mass Transfer*, 35 (2008), 10, pp.1327-1334
- [21] Promvong, P., Kwankaomeng, S., Periodic Laminar Flow and Heat Transfer in a Channel with 45° Staggered V-Baffles, *International Communications in Heat and Mass Transfer*, 37 (2010), 7, pp. 841-849
- [22] Promvong, P., Heat Transfer and Pressure Drop in a Channel with Multiple 60° V-Baffles, *International Communications in Heat and Mass Transfer*, 37 (2010), 7, pp. 835-840
- [23] Promvong, P., et al., Thermal Behavior in Solar Air Heater Channel Fitted with Combined Rib and Delta-Winglet, *International Communications in Heat and Mass Transfer*, 38 (2011), 6, pp. 749-756
- [24] Tandiroglu, A., Ayhan, T., Energy Dissipation Analysis of Transient Heat Transfer for Turbulent Flow in a Circular Tube with Baffle Inserts, *Applied Thermal Engineering*, 26 (2006), 2, pp. 178-185
- [25] Tandiroglu, A., Effect of Flow Geometry Parameters on Transient Heat Transfer for Turbulent Flow in a Circular Tube with Baffle Inserts, *International Journal of Heat and Mass Transfer*, 49 (2006), 9-10, pp. 1559-1567
- [26] Tandiroglu, A., Effect of Flow Geometry Parameters on Transient Entropy Generation for Turbulent Flow in Circular Tube with Baffle Inserts, *Energy Conversion and Management*, 48 (2007), 3, pp. 898-906
- [27] Singh, S., et al., CFD (Computational Fluid Dynamics) Investigation on Nusselt Number and Friction Factor of Solar Air Heater Duct Roughened with Non-Uniform Cross-Section Transverse Rib, *Energy*, 84 (2015), 5, pp. 509-517
- [28] Yang, W., Experimental Study on The Heat Transfer Characteristics of High Blockage Ribs Channel, *Experimental Thermal and Fluid Science*, 83 (2017), 5, pp. 248-259
- [29] Skullong, S., et al., Effects of Rib Size and Arrangement on Forced Convective Heat Transfer in a Solar Air Heater Channel, *Heat and Mass Transfer*, 51 (2015), 10, pp. 1475-1485
- [30] Sahel, D., et al., Enhancement of Heat Transfer in a Rectangular Channel with Perforated Baffles, *Applied Thermal Engineering*, 101 (2016), pp. May, 156-164
- [31] Sahel, D., et al., A Numerical Study of Fluid-flow and Heat Transfer over a Fin and Flat Tube Heat Exchangers with Complex Vortex Generators, *The European Physical Journal Applied Physics*, 78 (2017), 3, 34805
- [32] Kumar, R., et al., Comparative Study of Effect of Various Blockage Arrangements on Thermal Hydraulic Performance in a Roughened Air Passage, *Renewable and Sustainable Energy Reviews*, 81 (2018), 1, pp. 447-463
- [33] David Huang, K., et al., Experimental Study of Fluid-flow and Heat Transfer Characteristics in the Square Channel with a Perforation Baffle, *International Communications in Heat and Mass Transfer*, 35 (2008), 9, pp. 1106-1112
- [34] Karwa, R., Maheshwari, B. K., Heat Transfer and Friction in an Asymmetrically Heated Rectangular Duct with Half and Fully Perforated Baffles at Different Pitches, *International Communications in Heat and Mass Transfer*, 36 (2009), 3, pp. 264-268
- [35] Kumar, A., et al., Effect of Roughness width Ratio in Discrete Multi V-Shaped Rib Roughness on Thermo-Hydraulic Performance of Solar Air Heater, *Heat Mass Transfer*, 51 (2015), 2, pp. 209-220
- [36] Boukhadia, K., et al., Effect of the Perforation Design on the Fluid-flow and Heat Transfer Characteristics of a Plate Fin Heat Exchanger, *International Journal of Thermal Sciences*, 126 (2018), 4, pp. 172-180
- [37] Alem, K., et al., The CFD Investigations of Thermal and Dynamic Behaviors in a Tubular Heat Exchanger with Butterfly Baffles, *Frontiers in Heat and Mass Transfer (FHMT)*, 10 (2018), Mar., 27
- [38] Mellal, M., et al., Hydro-Thermal Shell-Side Performance Evaluation of a Shell and Tube Heat Exchanger under different Baffle Arrangement and Orientation, *International Journal of Thermal Sciences*, 121 (2017), 11, pp. 138-149
- [39] \*\*\*, Fluent Inc., (2005), User's Guide 6.2, Centerra Resource Park 10 Cavendish Court Lebanon, NH 03766
- [40] Incropera, F., Dewit, P. D., *Introduction Heat Transfer*, 5<sup>th</sup> ed., John Wiley and Sons Inc., New York, USA, 2006